Applied Ecology and Environmental Sciences, 2019, Vol. 7, No. 5, 176-181
Available online at http://pubs.sciepub.com/aees/7/5/3
Published by Science and Education Publishing
DOI:10.12691/aees-7-5-3

Graphene-CuO nanocomposite for Efficient Photocatalytic Reduction of *Pb (II)* under Solar Light Irradiation

B. Prashanti[1,*], I. Sreevani[2], B. Suresh[1], T. Damodharam[1]

[1]Department of Environmental Sciences, Sri Venkateswara University, Tirupati, 517 502, A.P., India
[2]Department of H & S, KSRM College of Engineering, Kadapa – 516005, A.P. India
*Corresponding author: prashantichandana123@gmail.com

Received September 20, 2019; Revised October 24, 2019; Accepted November 05, 2019

Abstract A facile synthesis of Graphene oxide-copper oxide nanocomposite (GO-CuO) was performed by using a wet chemical method by using graphene oxide and copper acetate precursors. There is no any other polymer or seed involved for preparation of nanocomposite The as-synthesized materials structure and morphology was calibrated by Powdered X-ray diffraction (P-XRD), and intercalated with Raman spectroscopy. Morphology features of GO-CuO nanocomposites were explored by FE-SEM, the quantitative and elemental analyses of as-synthesized materials were measured by electron dispersive spectroscopy (EDS), the size, shape, and orientation of as-synthesized catalysts were examined by transmission electron microscopy TEM with selective area electron diffraction. The results reveal that the nanocomposite with a size range from 5-10 nm uniformly anchored onto GO sheets and photocatalytic degradation of lead ion was studied by using a UV-VIS spectrophotometer. Significant high-performance photocatalytic activity of GO-CuO nanocomposite was exhibited on lead ions degradation under solar light.

Keywords: *Reduced graphene, GO-CuO nanocomposite, TEM, photocatalytic degradation*

Cite This Article: B. Prashanti, I. Sreevani, B. Suresh, and T. Damodharam, "Graphene-CuO nanocomposite for Efficient Photocatalytic Reduction of *Pb (II)* under Solar Light Irradiation." *Applied Ecology and Environmental Sciences*, vol. 7, no. 5 (2019): 176-181. doi: 10.12691/aees-7-5-3.

1. Introduction

Water pollution has been a vital environmental issue for the last few decades. Industrial organic dyes and heavy metals are considered to be the most important sources of water pollution and lead to acute and chronic health issues. A serious problem pertains to the contamination of water because of the hazardous materials from the plastic, leather and textile industries. Lead is one of the poisonous heavy metals released from various industrial processes, such as mining and processing plants. Due to the high toxicity of Pb(II) to the nervous, kidneys and reproductive systems, the United States Environmental Protection [1,2]. Agency (USEPA) and the World Health Organization (WHO) have regulated the maximum Pb(II) pollution levels in drinking water below 10 µg/L. Because the toxicity causes serious damage to the human body as well as the environment, the technology of Pb (II) ion removal from wastewater is urgently required by more and more stringent environmental regulations in each country [3,4,5].

Among them, adsorption seems to be the most attractive approach due to its recovery merit and easy handling. However, it is difficult to remove the total ions by sole adsorption due to an accompanying desorption process. For heterogeneous photocatalysis, the photocatalytic reaction is implemented by the excitation of electrons from the valence band to the conduction band of the semiconductor upon light irradiation, wherein the excited electrons and holes can be used in reduction and oxidation reactions, respectively [6,7,8,9]. Because the excited electrons are highly reductive, photocatalysis can be used in reductive or oxidative removal of heavy metal pollutants in water. For example, Chen and Ray [10] used Degussa P25 and Hombikat UV100 as the catalysts for photocatalytic removal of different heavy metal ions. In parallel, Stroyuk et al. studied photocatalytic Pb(II) reduction over ZnO and concluded that the accumulation of excited electrons could lead to the formation of cathodically polarized nanoelectrode and favored Pb(II) reduction although the photocatalytic Pb(II) reduction over ZnO was thermodynamically forbidden[11]. Liyuan et al[12] reported the Enhanced photocatalytic reduction of aqueous Pb(II) over Ag loaded TiO_2 with formic acid as a hole scavenger.

In recent years, there has been considerable research focus on uncovering the exceptional properties of graphene/CuO nanocomposites. Incorporating CuO nanostructures onto graphene can make new nanomaterials with improved properties [13,14,15,16]. The nanocomposites formed by the immobilization of CuO nanostructures on the two-

dimensional surface of graphene-based materials display significant variation in the performance as compared to CuO nanostructures [17,18]. Additional novel features can be introduced in the CuO nanostructures by functionalization and interaction or charge transfer between graphene and CuO nanostructures. Moreover, these multiphase materials possess a combination of individual features of constituents.

The aim of this work is the chemical modification of CuO by RGO to achieve the high-performance catalysis of Pb(II) under solar light irradiation. We target to exploit exceptional physical and chemical properties of RGO by synthesizing GO-CuO nanocomposite and hence to explore its performance in photocatalytic applications.

2. Materials and Methods

2.1. Materials

Natural graphite flakes were commercially obtained from Sigma-Aldrich. Besides, zirconium nitrate $(ZrNO_3)_2$ $2H_2O$, copper acetate dihydrate $[(CH_3COO)_2Cu.2H_2O]$, sulphuric acid (H_2SO_4), potassium manganese oxide ($KMnO_4$), sodium nitrate ($NaNO_3$), sodium hydroxide (NaOH), hydrogen peroxide (H_2O_2), hydrochloric acid (HCl) and all these chemicals procured from the Merck and used without further refinement and ethanol was supplied by China Medicine Co. Ltd. The double-distilled water was used for the total process.

2.2. Synthesis of Graphite Oxide

Graphite oxide was synthesized from graphite, using a modified Hummer's method [19]. In a typical procedure, about 5g of graphite powder was added to 115 mL of concentrated (98%) H_2SO_4 in an ice bath with stirring for 30 min. A 15 g of $KMnO_4$ was added slowly to the above mixture with stirring and cooling for 30 min. Subsequently, 2.5 g of $NaNO_3$ was added with continuous stirring for 1h. So that the temperature of the mixture maintained below 15^oC during that time. The temperature of the mixture then raised to 40°C with a water bath, and the mixture was continuously stirred for 30 min. After that, the mixture was diluted by 800~1000 mL of distilled water, the temperature of which then raised to 98 ^oC. The mixture was then added by H_2O_2 (30%) until gas evolution ceased followed by filtering. The color of the dispersion turned from black to yellow. The product was washed repeatedly with 1M HCl (5%) and distilled water until the pH value of the product arrived at near 7. Then the product was dried in an air oven at 60°C to obtain graphite oxide.

2.3. Synthesis of GO-CuO Nano Photocatalysts

In this work, we synthesis process of the GO-CuO nanocomposite reported in the previous study [20]. To prepare a colloidal suspension of GO, about 60 mg of as-prepared Graphite oxide was dispersed in 60 ml of ethanol by sonication for 1h. Consequently, copper acetate 0.25M was added into the dispersion and then add dropwise 1M of NaOH solution up to pH=10, which was calculated by pH meter. The total mixture was maintained at 140°C for 12 hours under an N_2 atmosphere. The product was washed several times with first by ethanol and thereafter distilled water. After that GO-CuO dried at 80°C overnight in a hot air oven. The synthesis procedure was shown in Figure 1.

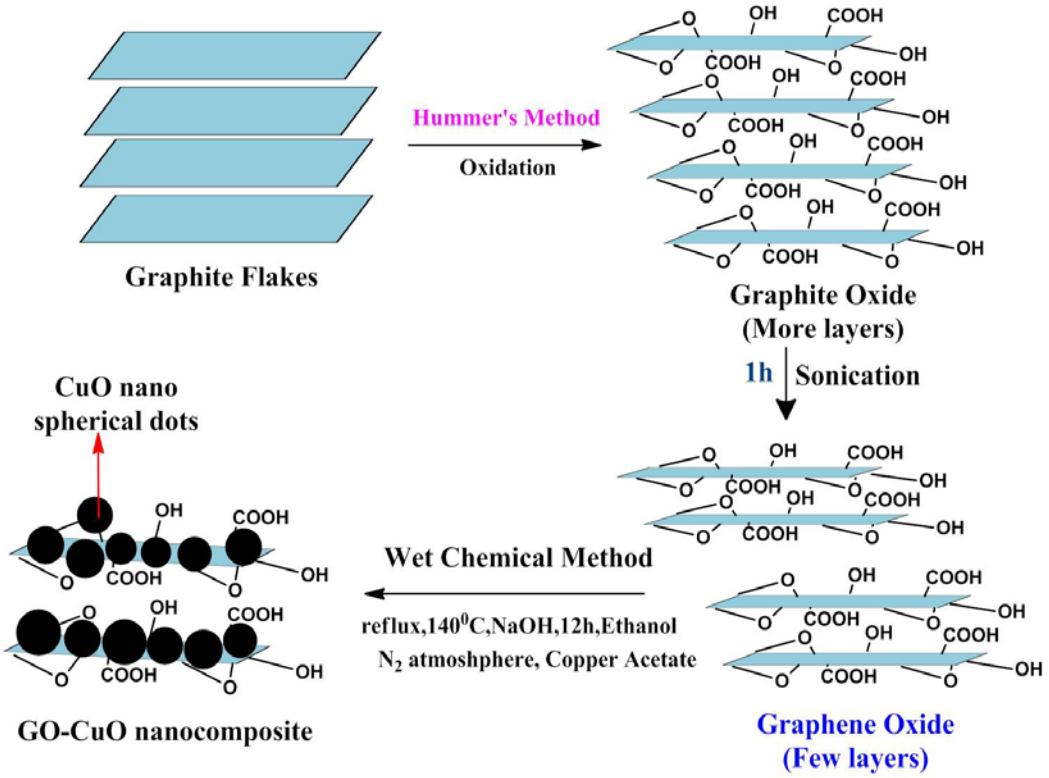

Figure 1. Chemical route synthesis of GO-CuO nanocomposites

2.4. Characterization

XRD patterns of the catalysts were recorded by X-ray diffractometry(XRD) Bruker D8 using CuKα 1(1.5406 Å) and Kα 2(1.54439 Å) radiations, Morphologies of as-obtained products were studied by Scanning Electron Microscope (SEM) imaging with energy dispersive Absorption X-ray spectroscopy (EDAX) or Energy dispersive spectrum (EDS) using a Carl Zeiss model Ultra 55 microscope operating at 5 and 20 kV, TEM images of the samples were collected on a Tecnai G2FEI F12 I at 200 kV, Carbon coated TEM grids were used before taking the images of the compounds. Raman spectra were recorded using a WiTec alpha 200 SNOM system. The pH of the solution was checked by using Elico pH meter.

2.5. Photocatalytic Activity Studies

The removal of the lead solution was evaluated by the adsorption–degradation efficiency of Pb(II) solution in dark and solar light irradiation. Pb(II) solutions (30 mL, 5×10^{-5} $molL^{-1}$) containing 30 mg of samples were sealed in a glass beaker and ultra-sonicated for 5 min, followed by magnetic stirring in dark for 30 min to ensure absorption–desorption equilibrium. After solar light illumination, 3 mL of samples were taken out at periodic time intervals (60 min) and separated through centrifugation. The clear supernatant solution was recorded as base concentration C_0. The supernatants were analyzed by recording variations of the absorption band maximum in the UV–vis spectra of Pb(II) by using a Shimadzu-1800 UV-visible Spectrometer to determine the concentration of Pb(II) at optical absorption at 475 nm, which denoted as C_t. In the photocatalytic degradation test, the decomposition rate could be calculated using the equation:

$$\ln\left(C / C_0\right) = k \times t$$

Here, C_0 is the pollutant concentration before sunlight irradiation, and C_t is the pollutant concentration in the solution after the photo-degradation, k was the decomposition rate constant, and t was the reaction time.

3. Results and Discussion

The crystalline nature and orientation of the as-synthesized Graphite oxide, CuO and GO-CuO nanocomposite were analyzed by powder X-ray diffraction (PXRD) as shown in Figure 2. For graphite oxide an intense crystalline peak around 9.92°. All the samples exhibit analogous diffraction peaks in terms of the CuO framework. The dominant peaks located at ca. 35.55, 46.26, 48.70, 53.54, 58.33, 61.55, 66.22 and 66.14° are indexed to ($\bar{1}11$), (111), (202), (020), (202), (113), (311) and (202) crystallographic planes of monoclinic CuO (JCPDS File Card No. 89-5899) consistent with GO-CuO composite. Where the diffraction peaks can be readily indexed to CuO with ($\bar{1}11$) and (111) planes confirm the presence of CuO in the composite catalyst [21]. The XRD pattern demonstrates the presence of a monoclinic phase of CuO with no indication of Cu_2O and $Cu(OH)_2$ phase. No characteristic diffraction peaks for GO are observed in the pattern because of the low amount and the relatively low diffraction intensity of GO.

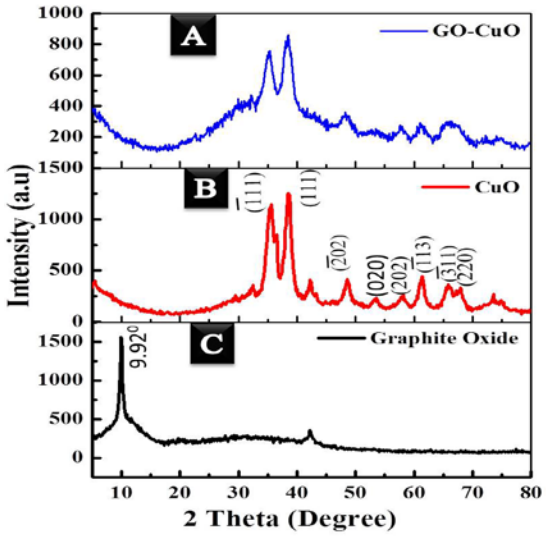

Figure 2. P-XRD pattern of the (A) GO-CuO and (B) CuO and (C) Graphite oxide

The Raman spectra of GO and GO-CuO composites are shown in (Figure 3). The D and G bands were observed in the range of 1000-2000 Cm^{-1}. Generally in GO-based samples, the disorder-induced D bands arise from the tangential stretch and sp3-hybridized carbon and the G band represents the crystalline graphite with E_{2g} zone center mode; moreover, the I_D/I_G ratio depends strongly on the amount of disorder in the graphitic material [22]. The I_D/I_G ratio should increase when more defects are introduced to GO. According to Figure 3, the I_D/I_G ratio of GO-CuO composite is 0.998 which is higher than the 0.990 calculated from GO. That is to say, CuO modification can be effective in bringing several defects into the structure of GO.

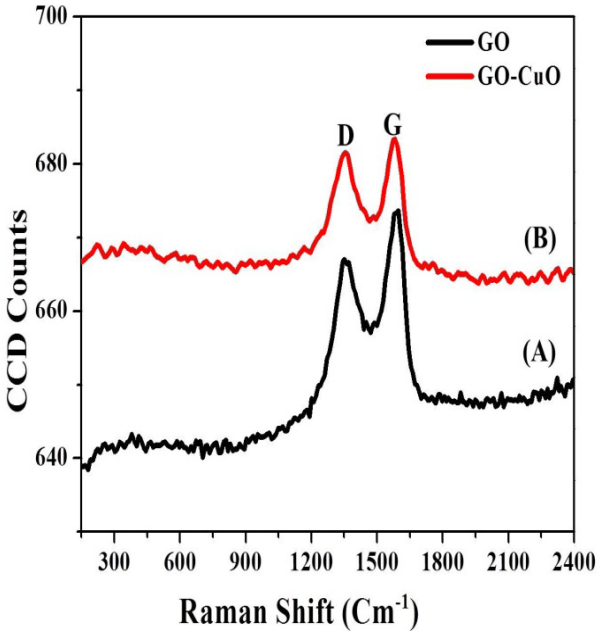

Figure 3. Raman measurements of (A) GO and (B) GO-CuO

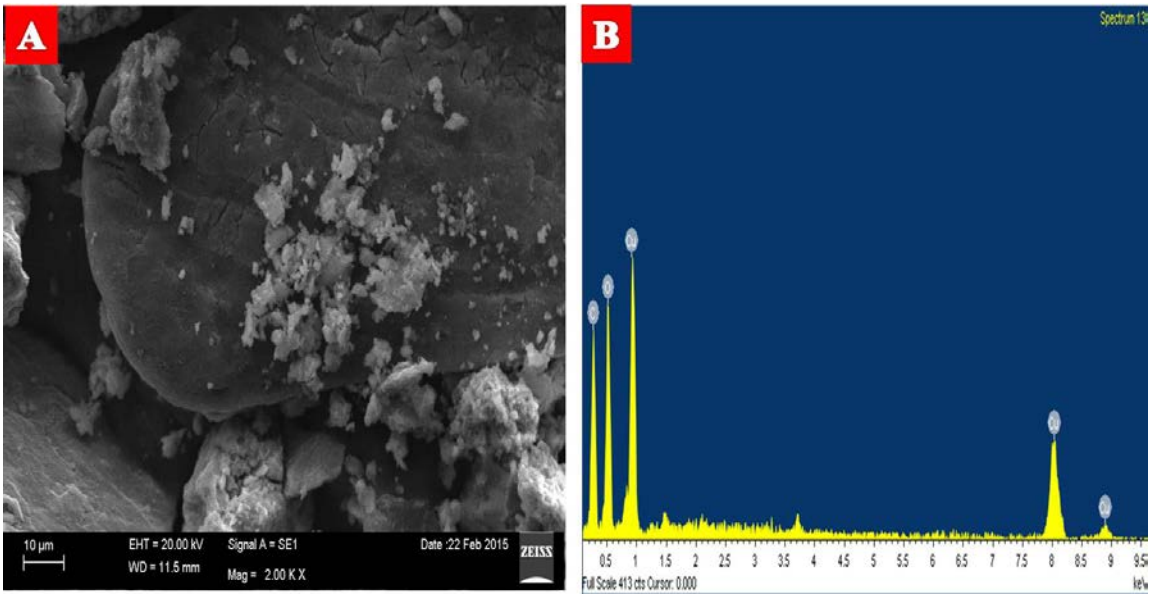

Figure 4. (A) SEM image and (B) EDS of GO-CuO composite

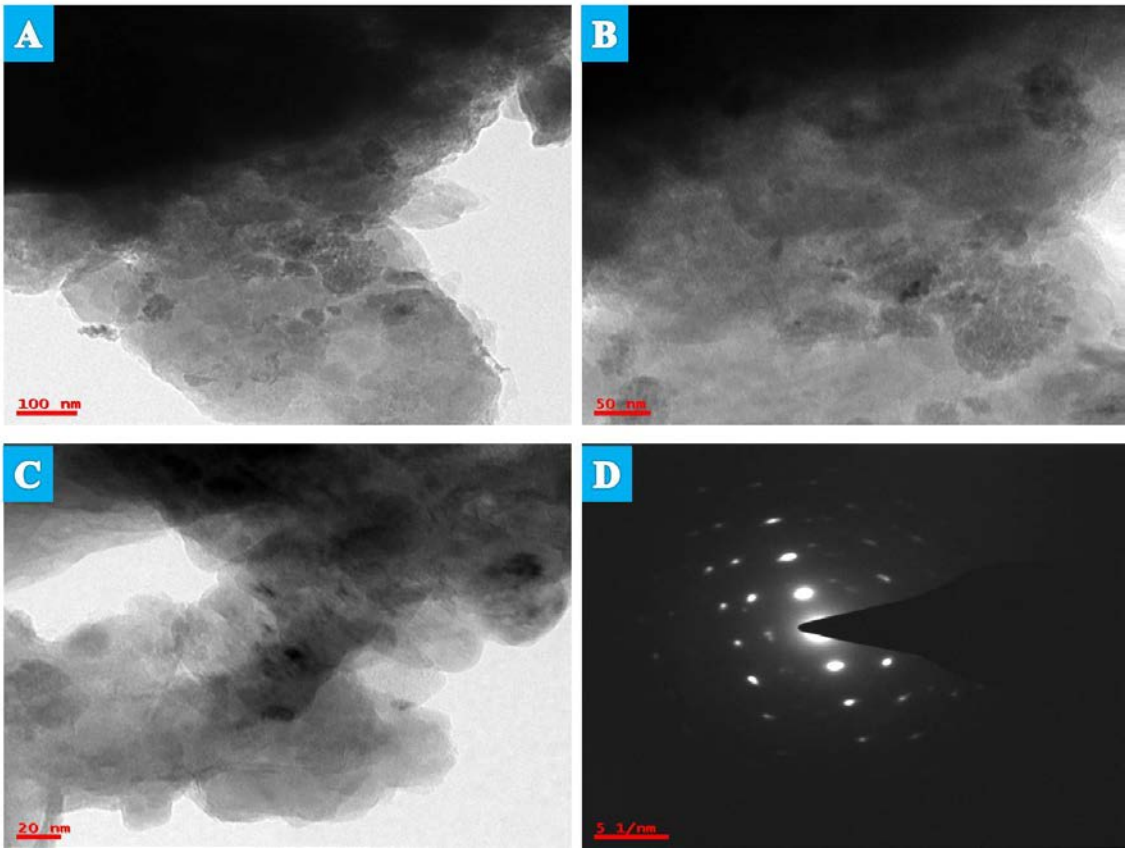

Figure 5. (A, B, C) TEM micrographs at different magnification and (D) SAED pattern of GO-CuO composite

The SEM of nanocomposite was taken as powder synthesized, images were taken on carbon tape. Figure 4. A shows the SEM images it is unambiguous that the morphology of intercalated nanocomposite particles is really in nanosize and it shows the clumsy morphology due to the aggregation of particles in the solution while synthesis. Figure 4.B shows the Energy-dispersive spectrum (EDS) results of the GO-CuO nanocomposite. Cu, O, C and Cu elements are observed.

Figure 5 A, B, C illustrate the typical TEM images of GO-CuO nanocomposite. It can be seen that the exfoliated GO sheet was decorated by spherical dot CuO, with a size <10 nm. Figure 5 D displays selective Area Electron diffraction (SAED) pattern of hybrid material shows the fusion of superlattices which are characteristic nature of the layer structure of any kind of materials.

The photocatalytic oxidation of Pb(II) in aqueous solution under the solar light irradiation was carried out at regular time intervals are shown in Figure 6a. The absorption spectra of these solutions decreased gradually with irradiation time. The intensity of the solar light is found to be around one lack of flux. The characteristic

absorption of Pb(II) almost disappeared after about 60 min, and the color of the Pb(II) solution changed gradually from pink to colorless with continuous light irradiation for 60 min. It is observed that Pb(II) cannot be oxidized under the dark condition even in the presence of photocatalyst GO-CuO composites exhibit better photocatalytic performance than pure CuO. At concentration 5×10^{-5} M of Pb(II) degradation is 98%, which shows the GO-CuO is a good catalyst**.** The CuO shows the degradation of Pb(II) removal is 42%, graphite oxide removal is 15% and mechanical mixing of GO+CuO is 60%. The GO-CuO composite material possesses much higher photocatalytic activity than pure CuO, GO and a mechanical mixture of GO+CuO. Figure 6b displays the UV-vis absorbance curves of degraded Pb(II) solutions at different solar light irradiation times.

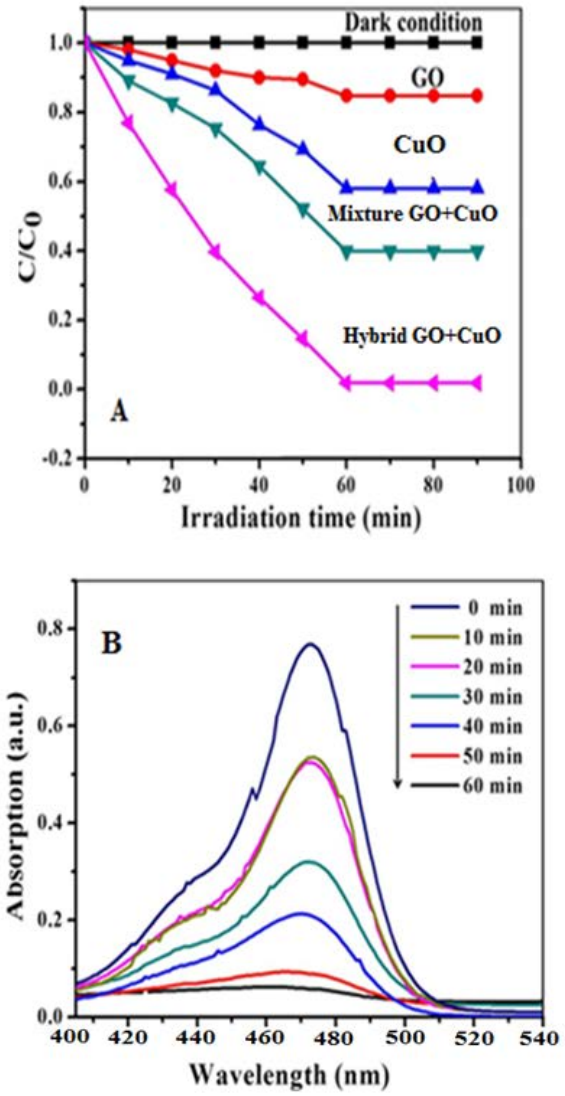

Figure 6. (a) The comparison studies of degradation of Pb(II) at different catalysts (b) The evolution of UV–vis spectra for Pb(II) solution during the photocatalysis process with GO-CuO under sun light irradiation

4. Conclusion

In conclusion, this work deals with a facile wet chemical method to fabricate CuO well doped and dispersed on GO sheets without any surfactants. The SEM, TEM shows that the GO-CuO nanocomposites were randomly anchored onto the graphene sheets. Photodegradation activity tests exposed that GO–CuO nanocomposites show superior catalytic efficiency for lead ion compared to bare Cuo, GO and mechanical mixture. This signifies that the electron transfer between GO and CuO will greatly hinder the recombination of photo-induced charge carriers and extends the lifetime of electrons, which keeps in the improvement of the lifetime of electrons of photocatalytic performance. Therefore, solar light-sensitive catalyst facilities are used for environmental applications.

Acknowledgments

We gratefully acknowledge the instrumental support of the University of Hyderabad.

References

[1] P.X. Sheng, Y.P. Ting, J.P. Chen, L. Hong, Sorption of lead, copper, cadmium, zinc, and nickel by marine algal biomass: characterization of biosorption capacity and investigation of mechanisms, J. Coll. Interf. Sci., 275, 131-141, 2004.

[2] M. Gavrilescu, Removal of heavy metals from the environment by biosorption, Eng. Life Sci. 4, 219-232, 2004.

[3] K. Yasukazu, K. Ryo, N. Takuya, S. Ryo, S. Kazunori, Improving Effect of MnO_2 Addition on TiO_2-Photocatalytic Removal of Lead Ion from Water, Journal of Water and Environment Technology, 15, 35-42, 2017.

[4] L. Murruni, F. Conde, G. Leyva, M. I. Litter, Photocatalytic reduction of Pb(II) over TiO_2: new insights on the effect of different electron donors, Applied Catalysis B, 84, 563–569, 2008.

[5] K. Kabra, R. Chaudhary, R. L. Sawhney, Treatment of hazardous organic and inorganic compounds through aqueous phase photocatalysis: a review, Industrial and Engineering Chemistry Research, 43(24), 7683-7696, 2004.

[6] Herrmann, J.M. Heterogeneous photocatalysis: fundamentals and applications to the removal of various types of aqueous pollutants, Catal. Today, 53, 115-129, 1999.

[7] M.R. Hoffmann, S.T. Martin, W. Choi, D.W. Bahnemann, Environmental applications of semiconductor photocatalysis, Chem. Rev., 95, 69-96, 1995.

[8] A.L. Linsebigler, G.Q. Lu, J.T. Yates, Photocatalysis on TiO_2 surfaces: principles, mechanisms, and selected results, Chem.Rev., 95, 735-758, 1995.

[9] M.I. Litter, Heterogeneous photocatalysis transition metal ions in photocatalytic systems. Appl. Catal. B: Environ., 23, 89-114, 1999.

[10] D. Chen, A. K. Ray, Removal of toxic metal ions from wastewater by semiconductor photocatalysis, Chem. Eng. Sci., 56(4), 1561-1570, 2001.

[11] A.L Stroyuk, V.V. Shvalagin, S.Y. Kuchmii, Photochemical synthesis and optical properties of binary and ternary metal-semiconductor composites based on zinc oxide nanoparticles. J. Photochem. Photobio. A: Chem., 173, 185-194, 2005.

[12] L. Liyuan, F. Jiang, J. Liu, H. Wan, Y. Wan, S. Zheng, Enhanced photocatalytic reduction of aqueous Pb(II) over Ag loaded TiO_2 with formic acid as hole scavenger, Journal of Environmental Science and Health-Part A, 47(3), 327-336, 2012.

[13] S. Dutta, K. Das, K. Chakrabarti, D. Jana, S.K. De, S. De, the Highly efficient photocatalytic activity of CuO quantum dot decorated rGO nanocomposites, Phys. D: Appl. Phys., 49, 315107-315115, 2016.

[14] N. Yusoff, N.M. Huang, M.R. Muhamad, S.V. Kumar, H.N. Lim, I. Harrison, Hydrothermal synthesis of CuO/functionalized graphene nanocomposites for dye degradation, Mater. Lett. 93, 393-396, 2013.

[15] Y.W. Hsu, T.K. Hsu, C.L. Sun, Y.T. Nien, N.W. Pu, M.D. Ger, Synthesis of CuO/graphene nanocomposites for nonenzymatic electrochemical glucose biosensor applications, Electrochim. Acta, 82, 152-157, 2012.

[16] Z. Zhang, P. Pan, X. Liu, Z. Yang, J. Wei, Z. Wei, 3D-Copper oxide and copper oxide/few-layer graphene with screen printed nanosheet assembly for ultrasensitive non-enzymatic glucose sensing, Mat. Chem. Phys., 187, 28-38, 2017.

[17] Y. Zhao, X. Song, Q. Song, Z. Yin, A facile route to the synthesis of copper oxide/reduced graphene oxide nanocomposites and electrochemical detection of catechol organic pollutant, Cryst Eng Comm, 14, 6710-6719, 2012.

[18] B. Wang, X.L. Wu, C.Y. Shu, Y.G. Guo, C.R. Wang, Synthesis of CuO/graphene nanocomposite as a high-performance anode material for lithium-ion batteries, J. Mater. Chem., 20, 10661-10664, 2010.

[19] J. Zhu, G. Zeng, F. Nie, X. Xu, S. Chen, Q. F. Han, X. Wang, Decorating graphene oxide with CuO nanoparticles in a water–isopropanol system. Nanoscale, 2, 988-994, 2010.

[20] B. Prashanti, T. Damodharam, Fabrication of Graphene–CuO Nanocomposite with Improved Photocatalytic Degradation for Palladium Solution under Solar Light Irradiation, Journal of Nanoscience and Technology, 4(5), 497-499, 2018.

[21] M. Suleiman, M. Mousa, A. Hussein, B. Hammouti, T. B. Hadda, I. Warad, Copper(II)-Oxide Nanostructures: Synthesis, Characterizations and their Applications–Review. J. Mater. Environ. Sci., 4 (5), 792-797, 2013.

[22] J. Song, L. Xu, C. Zhou, R. Xing, Q. Dai, D. Liu, H. Song, Synthesis of Graphene Oxide Based CuO Nanoparticles Composite Electrode for Highly Enhanced Nonenzymatic Glucose Detection. ACS Appl. Mater. Interfaces, 5, 12928-12934, 2013.